^{14}N Electron Spin−Echo Envelope Modulation of the $S = {}^3/_2$ Spin System of the *Azotobacter vinelandii* Nitrogenase Iron−Molybdenum Cofactor†

Hong-In Lee,‡ Kristin S. Thrasher,§ Dennis R. Dean,*,§ William E. Newton,*,§ and Brian M. Hoffman*,‡

Department of Chemistry, Northwestern University, Evanston, Illinois 60208, and Department of Biochemistry, Virginia Polytechnic Institute and State University, Blacksburg, Virginia, 24061

Received April 28, 1998; Revised Manuscript Received July 20, 1998

ABSTRACT: Wild-type nitrogenase MoFe protein shows a deep ^{14}N electron spin−echo envelope modulation (ESEEM) arising from a nitrogen nucleus (N1) coupled to the $S = {}^3/_2$ spin system of the FeMo-cofactor of the MoFe protein. A previous ESEEM study on altered MoFe proteins generated by substitutions at the α-195-histidine position suggested that α-195-histidine provides a hydrogen bond to the FeMo-cofactor but is not the source of the ^{14}N1 modulation [DeRose et al. (1995) *Biochemistry 34*, 2809−2814]. This study also raised the possibility of a correlation between ESEEM spectroscopic properties and the nitrogenase phenotype. We now report ESEEM studies on altered MoFe proteins with substitutions at residues α-96-arginine, α-359-arginine, and α-381-phenylalanine to (i) assign the first-shell hydrogen bonding as revealed by the ^{14}N modulation; (ii) explore the mechanistic relevance of the ESEEM signatures to nitrogenase activity; and (iii) study microscopic changes within the polypeptide environment of the FeMo-cofactor. Present ESEEM data reveals that two kinds of ^{14}N modulations are present in wild-type MoFe protein. A new 2-dimensional procedure for high-precision analysis of the ESEEM data of the MoFe proteins shows that the deep wild-type ESEEM modulation (denoted N1) has a hyperfine-coupling constant of $A_{iso} = 1.05$ MHz and nuclear quadrupole coupling parameters of $e^2qQ = 2.17$ MHz, $\eta = 0.59$; the other (denoted N2) has a smaller hyperfine coupling of $A_{iso} = \sim 0.5$ MHz and $e^2qQ = \sim 3.5$ MHz, $\eta = \sim 0.4$. The N2 ESEEM pattern is more obvious when unmasked by substitutions that result in the loss of the deep N1 modulation. Correlations of the ESEEM properties and catalytic activities of the altered MoFe proteins suggest that (i) the side chain of the α-359-arginine is the source of the deep ESEEM N1 modulation; (ii) one or both of the amide nitrogens of α-356-glycine/α-357-glycine are responsible for the weak N2 modulation; (iii) substitution of the nonpolar α-381-phenylalanine residue, as well as substitution of either the α-195-histidine or α-359-arginine residues, can eliminate the N1 interaction with FeMo-cofactor; and (iv) ESEEM can be used to detect slight reorientations of FeMo-cofactor within its polypeptide pocket, although the mechanistic relevance of the loss or perturbation of the hydrogen-bonding interactions between FeMo-cofactor and polypeptide environment has not yet been established.

Nitrogenase is the complex, two-component metalloenzyme that catalyzes biological nitrogen fixation. The individual nitrogenase component proteins are commonly referred to as the Fe protein and the MoFe protein, and these designations reflect the metal compositions of their respective metalloclusters. The Fe protein is a homodimer that serves as a nucleotide-dependent reductant of the MoFe protein. The Fe protein's redox-active species is a $[Fe_4S_4]$ cluster that is symmetrically bridged between the identical subunits. The MoFe protein is an $\alpha_2\beta_2$ heterodimer that contains two metallocluster types called the P-cluster and FeMo-cofactor. The P-cluster is an Fe_8S_7 cluster (*1, 2*) that is probably the primary acceptor of electrons delivered by the Fe protein (*3*−*5*), whereas FeMo-cofactor provides the site of substrate binding and reduction (*6, 7*). Our current understanding of how electrons are shuttled through the nitrogenase components to achieve N_2 reduction has been recently reviewed (*8*−*10*).

FeMo-cofactor consists of a metal-sulfur framework ($MoFe_7S_9$) and one molecule of (*R*)-homocitrate (Figure 1a) (*1, 11*). This framework is constructed from S-bridged $MoFe_3S_3$ and Fe_4S_3 cluster subfragments. Homocitrate is coordinated to the Mo atom through its β-hydroxy and β-carboxy groups. Crystallographic analyses have shown that the cofactor is buried within the MoFe protein α-subunit and is covalently attached to the protein by residues α-275-cysteine and α-442-histidine (residue numbers refer to the primary sequence of the *Azotobacter vinelandii* MoFe protein α-subunit). The former provides a thiolate ligand to Fe1 at one end of the cofactor and the latter binds the Mo atom through a side-chain nitrogen (N_δ) at the opposite end. Although α-275-cysteine and α-442-histidine provide its only covalent ligands, FeMo-cofactor is tightly packed within the MoFe protein α-subunit by (i) residues that approach each

† This work was supported by the NSF (MCB-9507061 to B.M.H. and MCB-9630127 to D.R.D.), the USDA (97-35305-4879 to B.M.H.), and the NIH (DK-37255 to W.E.N).

* To whom correspondence should be addressed.

‡ Northwestern University.

§ Virginia Polytechnic Institute and State University.

S0006-2960(98)00956-8 CCC: $15.00
Published on Web 09/05/1998

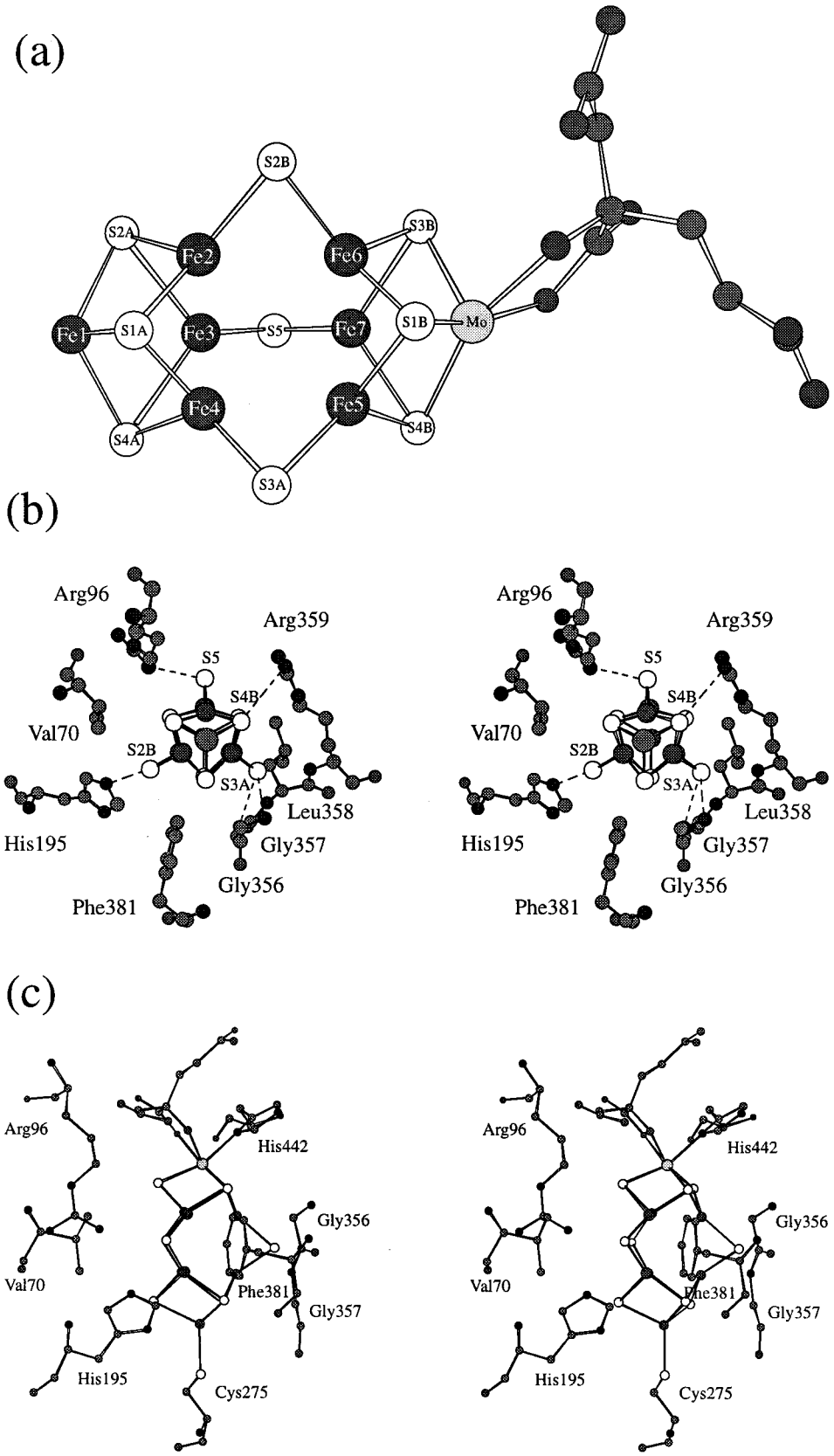

FIGURE 1: (a) The FeMo-cofactor of the MoFe protein from *Azotobacter vinelandii.* (b) Stereoscopic view of the FeMo-cofactor and selected residues viewed along the 3-fold axis of the cofactor. Dashed lines represent the possible hydrogen bonds revealed from the X-ray crystal structure. (c) Stereoscopic side view of the FeMo-cofactor and selected residues. All the figures are regenerated by using Chem 3D from the atomic coordinates (*11, 38, 39*) obtained from Brookhaven Database.

of its three faces (α-70-valine, α-359-arginine, and α-381-phenylalanine), (ii) residues that have the potential to hydrogen bond to the bridging sulfides (α-96-arginine, α-195-histidine, α-356-glycine, and α-357-glycine), and (iii) a residue that has the potential to hydrogen bond to a *S* atom contained within the $MoFe_3S_3$ subcluster fragment (α-359-

arginine). The spatial arrangement of these residues in relation to FeMo-cofactor is shown in Figure 1, panels b and c, and we refer to them as providing the "first shell" of polypeptide interactions with the FeMo-cofactor.

Prior to the availability of structural models, electron spin−echo envelope modulation (ESEEM) spectroscopy (*12*) had provided evidence for a N-atom coupled to the $S = {}^3/_2$ spin system of FeMo-cofactor (*13*). It was originally suggested that the N modulation might arise from a histidine residue that is covalently attached to the cofactor. This possibility was supported by the observation that the characteristic ESEEM signature of the *A. vinelandii* MoFe protein could be eliminated by substitution of α-195-histidine by an asparagine (*14*). However, subsequent structural studies revealed α-195-histidine is not covalently attached to the FeMo-cofactor, although it is within hydrogen-bonding distance of a central bridging sulfur (*1, 11*). Moreover, it was later shown that substitution of α-195-histidine by glutamine, rather than asparagine, has no affect on the ESEEM signature (*15*). Another feature, which distinguishes the altered α-195-asparagine MoFe protein from the altered α-195-glutamine MoFe protein, is that the former can neither bind nor effectively reduce N_2, whereas the latter binds, but does not effectively reduce, N_2 (*16, 17*). These observations led to the following questions. First, if α-195-histidine does not provide the interaction that gives rise to the characteristic ESEEM signature, which residue in the first shell does? Second, is the ESEEM signature diagnostic of the MoFe protein's ability to bind N_2 and, therefore, of potential mechanistic relevance? Third, is there more than one source of N-modulation within the ESEEM signature? Fourth, is it possible to perturb the ESEEM signature(s) by substitution of nonpolar R-groups that appear to have a role in positioning FeMo-cofactor within the polypeptide pocket? In the present study, we have addressed these questions by determining the ESEEM parameters of altered MoFe proteins having substitutions for individual amino acids that comprise the FeMo-cofactor's first shell of polypeptide interactions.

EXPERIMENTAL PROCEDURES

Mutant Strain Constructions and Biochemical Manipulations. Methods for oligonucleotide synthesis and use, site-directed mutagenesis, gene replacement, and the isolation of *A. vinelandii* mutant strains were performed as described previously (*16, 18, 19*). Each altered MoFe protein is designated by the name of the subunit (α in this case), the number of the amino acid position substituted, followed by the three-letter code for the substituting amino acid in superscript form, e.g., the altered MoFe protein having the α-195-histidine residue substituted by glutamine is designated as α-195^{Gln}. Strains are designated by DJ numbers. All mutants were derived from DJ527 which has an insertion mutation within *hoxKG* that abolishes its uptake hydrogenase activity without affecting any of the *nif* genes (*16*). Large-scale culture of *A. vinelandii*, media, crude extract preparation, MoFe protein purification, protein quantitation, and nitrogenase activity assays were performed as described or cited by Shen et al. (*20*). The altered MoFe protein (α-195^{Asn}) produced by mutant strain DJ528 has not yet been purified to homogeneity in an active form and was, therefore, only partially purified as described by Kim et al. (*16*). Additional strains were constructed that have either α-359-arginine substituted by glutamine or α-442-histidine substituted by asparagine and cysteine. None of these strains exhibited either catalytic activity or any $S = {}^3/_2$ EPR signal in crude extracts. However, the α-359^{Gln} MoFe protein was purified extensively and found to have a very low Mo content and only about 50% of the Fe content compared with wild-type. It was still completely inactive both catalytically and spectroscopically (data not shown).

Spectroscopic Procedures. Electron paramagnetic resonance (EPR) spectra were collected in dispersion mode under rapid-passage conditions (*21, 22*) at 2K on a modified Q-band (35 GHz) Varian E-110 spectrometer equipped with a liquid helium immersion dewar (*23*). ESEEM experiments were performed on a locally built X-band (9 GHz) pulsed EPR spectrometer (*24*). For ESEEM analysis of wild-type and altered MoFe proteins, a three-pulse echo (stimulated echo) sequence ($^{\pi}/_2 - \tau - {}^{\pi}/_2 - T - {}^{\pi}/_2$) was employed at 2K (*12*). The typical $^{\pi}/_2$ microwave pulse duration was 16 ns with power of ~1 W. The stimulated echo amplitudes were recorded by varying the time interval, *T*, between the second and the third pulses to construct the time-domain ESEEM data. The frequency-domain spectra were obtained through Fourier transformation (FT) of the time-domain data by modifying the "dead-time reconstruction" procedure originally developed by Mims (*25*).

The EPR spectrum of the FeMo-cofactor of the MoFe protein arises from the lower doublet of a zero-field split $S = {}^3/_2$ state. This doublet can be treated as if it has a fictitious spin of $S' = 1/2$ with principal g values of $\mathbf{g}' = (4.33, 3.77, 2.01)$. Although all the simulations were done in the fictitious spin representation as described elsewhere (*26*), the hyperfine tensors reported here are those that characterize the electron−nuclear interaction when described in the true ($S = {}^3/_2$) representation (A_{int}) (*27, 28*). The nuclear quadrupole parameters, which are independent of the electron spin representation, are reported as the quadrupole coupling constant (e^2qQ) or $K = e^2qQ/4$ and the asymmetry parameter (η).

^{14}N ESEEM spectra of the nitrogenase MoFe protein (Figure 2, panels d−f) present a four-line pattern similar to the well-known ^{14}N ESEEM often detected for "near cancellation" conditions. The peaks assigned to ν_1, ν_2, and ν_3 arise from the electron spin manifold where the nuclear Zeeman and the hyperfine interactions are opposed and characterized by the inequality, $w = \nu_{ef-}/K = |\nu_N - |A/2||/K < 1$. Here, ν_1, ν_2, and ν_3 closely correspond to zero-field nuclear quadrupole transitions ($\nu_2 + \nu_3 = \nu_1$) since the nuclear states in this manifold are mostly nuclear quadrupole states. The other spin manifold, where the nuclear Zeeman and the hyperfine interaction are added ($w_+ = \nu_{ef+}/K = |\nu_N + |A/2||/K > 1$), gives only one observable peak corresponding to a double quantum transition (denoted ν_{dq}) (*12*). We found that the simple analytical method of Astashkin et al. (*29*), which has been used to derive the ^{14}N nuclear hyperfine and quadrupole coupling parameters for "near cancellation" conditions, is not applicable for ESEEM when the observed $\mathbf{g}'$ and $\mathbf{A}'$ tensors are highly anisotropic as in

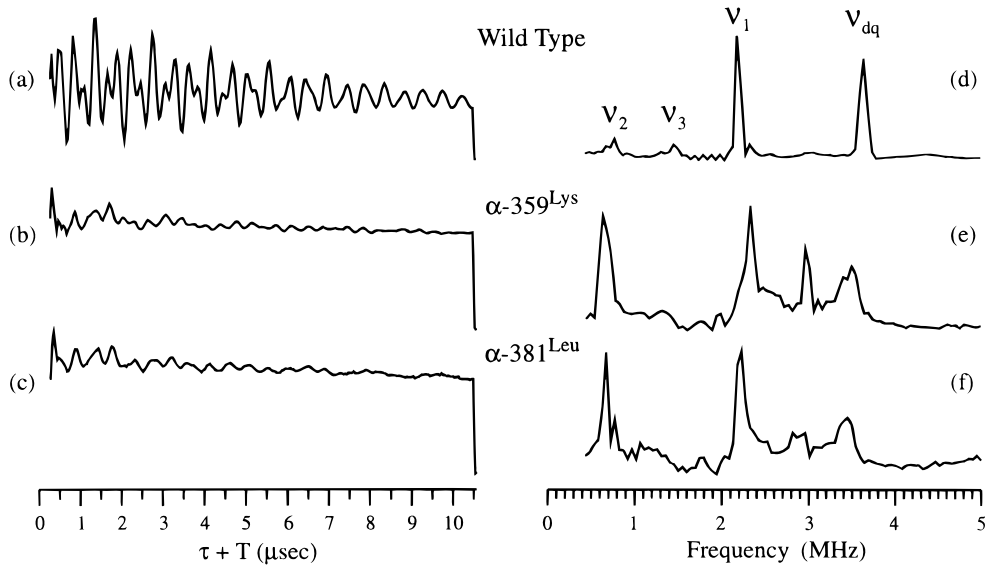

FIGURE 2: Three-pulse ESEEM time-domain and corresponding frequency-domain (FT) spectra at $g = 4.3$ of (a, d) wild-type, (b, e) α-359^{Lys}, and (c, f) α-381^{Leu} MoFe proteins. Experimental conditions: (a) field strength, 1594 G; microwave frequency, 9.547 GHz; $\tau =$ 148 ns; average, 1300 transients, (b) field strength, 1606 G; microwave frequency, 9.650 GHz; $\tau = 148$ ns; average, 2200 transients, and (c) field strength, 1597 G; microwave frequency, 9.611 GHz; $\tau = 148$ ns; average, 1760 transients. Other parameters are described in Experimental Procedures.

Table 1: EPR, ^{14}N ESEEM Patterns, and Substrate-Reduction Properties of Wild-Type and Altered MoFe Proteins

strain (MoFe protein)[b]	EPR[a]				ESEEM pattern[d]	substrate-reduction properties, product formation[e]		
	no. of signals[c]	g_1	g_2	g_3		NH_3	C_2H_4	H_2
DJ527 (wild-type)	1	4.33	3.77	2.01	N1	1204	2243	2596
DJ1310 (α-96^{Lys})	2	4.43	3.58	1.99	N1	373	804	972
		4.18	3.66	2.01				
DJ913 (α-96^{Gln})	1	4.37	3.66	2.01	N1	300	587	770
DJ528 (α-195^{Asn})[f]	1	4.27	3.78	2.01	$N2_a$	[f]		
DJ540 (α-195^{Gln})	1	4.36	3.64	2.01	N1	0	1282	1334
DJ987 (α-359^{Lys})	1	4.34	3.68	2.02	$N2_a$	709	1523	1587
DJ1036 (α-381^{Leu})	1	4.26	3.71	2.01	$N2_b$	816	1656	1844
DJ989 (α-381^{Ile})	2	4.24	3.72	2.01	$N2_b$	746	1812	1910
		4.57	3.43					

[a] The g-values are in the fictitious spin $S' = {}^1/_2$ (see text). Limits of the uncertainties of g-values are ±0.02 for g_1 and g_2 and ±0.01 for g_3. [b] Altered α-442^{Asn} (DJ859), α-442^{Cys} (DJ952), and α-359^{Gln} (DJ972) MoFe proteins show neither $S = {}^3/_2$ EPR signal nor catalytic activity. [c] The number of different $S = {}^3/_2$ EPR-active species observable. [d] The indicated ESEEM patterns refer to the three different ESEEM patterns discussed in the text and which are shown in Figures 3 and 4. [e] Product formation is indicated as the nanomoles of product formed per minute per milligram of purified protein. For NH_3 formation, the samples were assayed under a 100% N_2 atmosphere. For C_2H_4 formation, the samples were assayed under a 10% acetylene/90% Ar atmosphere. For H_2 production, the samples were assayed under a 100% Ar atmosphere. [f] For strain DJ528, the α-195^{Asn} MoFe protein was found to be unstable during the standard purification protocol, so activities for purified protein could not be reliably reported. Crude-extract assays for the α-195^{Asn} protein previously reported by Kim et al. (*16*) show that it has no N_2-reduction activity, approximately 8% of the wild-type C_2H_2-reduction activity, and approximately 20% of the wild-type proton-reduction activity. The α-195^{Asn} MoFe protein is also able to reduce C_2H_2 by four electrons to yield C_2H_6, but neither the wild-type nor any of the other altered MoFe proteins examined in this study could reduce C_2H_2 to C_2H_6. The ^{14}N ESEEM pattern for the α-195^{Asn} protein was determined using a partially purified sample as described by Kim et al. (*16*) and DeRose et al. (*15*).

the MoFe protein.[1] Instead, a 2D-pattern was obtained by collecting ESEEM spectra across the EPR envelope to achieve angle-selective ESEEM whose analysis yields the ^{14}N hyperfine and nuclear quadrupole tensors with respect to **g**-tensor (*30*). In that procedure, we first extracted the ^{14}N nuclear hyperfine and quadrupole coupling parameters by comparing measured frequencies to analytical solutions derived from Muha's solution for the eigenvalue problem of $I = 1$ (*31*) under the assumption of coaxial **g**, hyperfine, and nuclear quadrupole tensors. The interaction tensors and their orientations were then adjusted to fit the ESEEM spectra collected across the EPR envelope as described in detail elsewhere (*32*).

RESULTS

Diazotrophic Growth and Catalytic Activities of Mutant Strains. Table 1 lists a summary of the mutant strains characterized in the present study and the catalytic activities of their altered MoFe proteins. Mutant strains having MoFe proteins with substitutions at the α-442-histidine residue exhibit neither catalytic activity nor an $S = {}^3/_2$ EPR signal. The strain with a MoFe protein having residue α-359-arginine replaced by glutamine was similarly inactive. Thus,

[1] For example, for a hyperfine tensor which is coaxial with the zero-field splitting tensor, the observed hyperfine tensor, **A′**, is given by **A′** = ($g_1'A_1/g_e$, $g_2'A_2/g_e$, $g_3'A_3/g_e$). Thus, even an intrinsically isotropic hyperfine interaction becomes highly anisotropic for rhombic **g′** (*26*−*28*).

these altered MoFe proteins could not be characterized. Among the other mutants, only those having substitutions at the α-195-histidine position were unable to grow diazotrophically. Even though the MoFe protein produced by these particular mutants exhibited no significant N_2-fixing ability, they still retained a range of acetylene- and proton-reduction activities (Table 1) (*16, 17*). All of the other mutants characterized were capable of diazotrophic growth and produced a MoFe protein that retained significant levels of N_2-fixing capacity, as well as acetylene- and proton-reduction activities (Table 1). All of the altered MoFe proteins characterized in the present work retained an $S = {}^3/_2$ EPR signature that is similar to the wild-type MoFe protein (Table 1) so they were all amenable to the EPR and ESEEM spectroscopic analyses described below. Furthermore, because all of the altered MoFe proteins exhibited appreciable catalytic activities for both acetylene and proton reduction, plus a significant $S = {}^3/_2$ EPR signal, it is unlikely that any of the amino acid substitutions elicited global structural changes within the altered MoFe proteins.

Spectroscopic Features of Altered MoFe Proteins. The EPR spectrum of the MoFe protein arises from the lower doublet ($m_s = \pm{}^1/_2$) of the $S = {}^3/_2$ FeMo-cofactor. This spectrum can be represented by a fictitious spin $S' = {}^1/_2$ characterized by a $\mathbf{g}'$-tensor that is coaxial with the zero-field spitting tensor and has principal values of $\mathbf{g}'_{1,2,3} =$ (4.33, 3.77, 2.01) (hereafter, the prime is omitted for convenience). Table 1 lists the **g**-tensor values observed for the wild-type and altered MoFe proteins. As seen in the table, the g_1 and g_2 values of the altered MoFe proteins that retained an $S = {}^3/_2$ signal differ only slightly from those of the wild-type, whereas the g_3 values are unchanged. Thus, the electronic structure of the cofactor is conserved in all of the altered MoFe proteins examined. Two of the altered MoFe proteins (α-381^{Ile} and α-96^{Lys}), however, exhibit two similar sets of EPR signals, indicating that the FeMo-cofactor contained within these MoFe proteins is present in two slightly different orientations and/or polypeptide conformations. A similar situation was previously reported for an altered MoFe protein for which the α-277-arginine residue was substituted by histidine (*20*).

Figure 2 shows the "single crystal-like" ESEEM time-domain spectra and their corresponding frequency-domain (Fourier transformed, FT) spectra taken at $g_1 = 4.3$ for the wild-type and two of the altered MoFe proteins (α-359^{Lys} and α-381^{Leu}). The ESEEM of the wild-type MoFe protein shows a deep modulation (amplitude ≈ 90% of the electron-spin echo) arising from a ^{14}N nucleus that is coupled to the electron spin of the FeMo-cofactor (Figure 2a). The ^{14}N nucleus responsible for this modulation is hereafter designated as N1. The FT spectrum of the wild-type modulation shows two sharp and strong peaks at $\nu_1 = 2.24$ and $\nu_{dq} = 3.65$ MHz. Very weak features are also seen at $\nu_2 = 0.78$ and $\nu_3 = 1.46$ MHz (Figure 2d). The ^{14}N ESEEM of N1 in the wild-type MoFe protein at g_1 and g_2 was previously analyzed to give an intrinsic ^{14}N hyperfine coupling that is mostly isotropic ($\mathbf{A}_{int} = \sim$(0.9, 0.9, 1.2) MHz; $A_{iso} = 1$ MHz; point-dipole distance = 4 Å), a nuclear quadrupole coupling constant of $e^2qQ = 2.2$ MHz, and an asymmetry parameter of $\eta = 0.5$ (*15*). In contrast to the wild-type MoFe protein, the ESEEM for both α-359^{Lys} and α-381^{Leu} MoFe proteins exhibit dramatically diminished modulation amplitudes (modulation depth less than 15% of the electron-spin echo; Figure 2, panels b and c). In the FT spectrum of the α-359^{Lys} MoFe protein, four peaks are resolved at 0.65 (ν_2), 2.33 (ν_3), 2.98 (ν_1), and 3.50 (ν_{dq}) MHz with some minor features between 1 and 2 MHz (Figure 2e). The α-381^{Leu} MoFe protein shows essentially the same ESEEM features as α-359^{Lys} but with slight differences in peak positions: 0.68 (ν_2), 2.23 (ν_3), ∼2.9 (ν_1), and 3.44 (ν_{dq}) MHz (Figure 2f). These peaks also arise from a ^{14}N nucleus interacting with the cofactor and are respectively designated as $N2_a$ for the α-359^{Lys} spectrum, and as $N2_b$ for the α-381^{Leu} spectrum.

As described in Experimental Procedures, full characterization of the ^{14}N coupled to the spin of the FeMo-cofactor requires the analysis of a two-dimensional ESEEM data set across the EPR envelope (2D ESEEM). One such data set for wild-type MoFe protein is shown in Figure 3a. The N1 FT spectra show four features running across the EPR envelope (shaded in the figure). The ν_2 band shifts from ∼0.8 MHz ($g_1 = 4.3$) to ∼1.2 MHz ($g_3 = 2.0$). It has the broadest width at $g_2 = 3.8$, where it has contributions from the broadest range of molecular orientation with respect to the external magnetic field. The ν_3 band shifts from ∼1.5 MHz (g_1) to ∼1.2 MHz (g_3) and increases in relative intensity. The ν_2 and ν_3 bands appear to cross at $g = \sim 2.3$. The other bands, ν_1 and ν_{dq}, do not show much change of their frequency positions across the EPR envelope but their line shapes change due to the orientation selection. The procedure for this sort of analysis of a 2-D ESEEM data set is briefly discussed above and is detailed elsewhere (*32*). Figure 3b shows the simulation as a 2-D contour map of intensity as a function of frequency and g-value. The simulation was performed with the hyperfine tensor of $\mathbf{A}_{int} =$ (0.98, 1.02, 1.14) MHz, the nuclear quadrupole coupling constant of $e^2qQ = 2.17$ MHz, and $\eta = 0.59$ (Table 2). In the simulation, **g**, hyperfine, and nuclear quadrupole coupling tensors are coaxial. The parameters used for N1 are in agreement with those previously reported (*15*) but are much more accurately determined.

In Figure 4, 2D ESEEM data sets taken across the EPR envelopes of the altered α-359^{Lys} and α-381^{Leu} MoFe proteins are shown. The loss of N1 modulation for these two altered MoFe proteins corresponds to a complete loss of the wild-type peaks in the ESEEM frequency domain spectra (Figure 2). However, careful examination of the wild-type FT spectra reveals that the peaks observed for the altered α-359^{Lys} and α-381^{Leu} MoFe proteins are also present at low intensity in the wild-type ESEEM. Thus, this N2 interaction was first recognized in the α-359^{Lys} and α-381^{Leu} MoFe proteins as a consequence of their loss of the N1 interaction with the FeMo-cofactor. In other words, loss of the N1 interaction with FeMo-cofactor unmasks the ESEEM signature of the N2. N2 modulation of the FeMo-cofactor results in a frequency-domain pattern having four major features across the EPR envelope (shaded in the figure) and whose field dependence is similar, but not identical, for both altered proteins. In addition, other minor features are seen in the ESEEM spectra of these altered MoFe proteins but they occur with greater intensity in the α-359^{Lys} MoFe protein. These minor features might indicate the presence of yet another ^{14}N nuclear interaction with the spin center of FeMo-cofactor. It cannot be ascertained if this third ^{14}N modulation also occurs in the wild-type MoFe protein

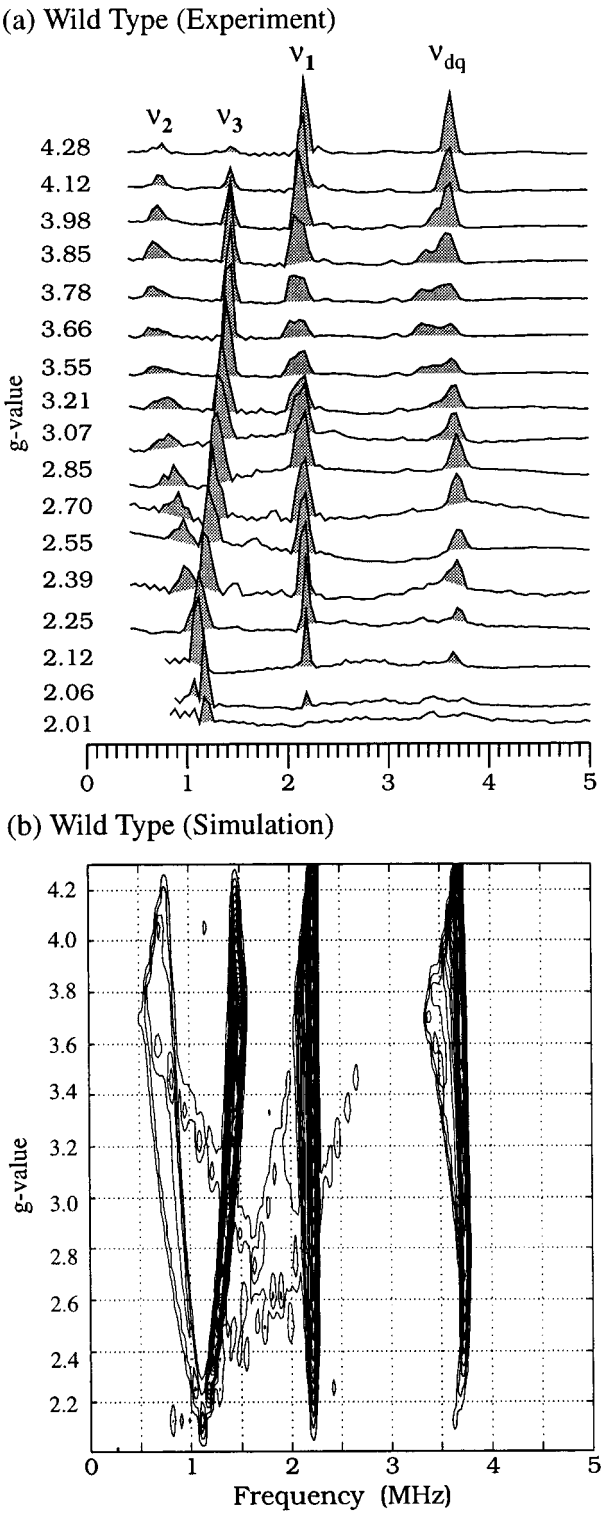

FIGURE 3: (a) Field-dependent three-pulse ESEEM FT spectra obtained across the EPR spectrum of wild-type MoFe protein and (b) corresponding simulation. Experimental conditions: microwave frequency, 9.547 GHz; τ = 124−152 ns. Simulation parameters are in Table 2 with τ = 150 ns and a Gaussian line width of 0.05 MHz. The simulation procedure is briefly described in Experimental Procedures.

because the modulation is very weak when compared to that of N1.

2D intensity contour maps (Figure 4, panels b and d) show the corresponding simulations for the major features of $N2_a$ and $N2_b$, respectively, for the altered α-359^{Lys} and α-381^{Leu} MoFe proteins. These simulations reveal that the hyperfine and the nuclear quadrupole coupling constants for N2 in both of the altered MoFe proteins are roughly the same: A_{iso} = ∼0.5 MHz, e^2qQ = ∼3.5 MHz, η = ∼0.4, although there are significant differences (Table 2). This result indicates that the same ^{14}N species probably gives rise to the modulation for both altered MoFe proteins, but that their structural environments are slightly different. Such nuclear quadrupole coupling parameters of e^2qQ = 3.0−3.5 MHz and η = ∼0.5 have been reported for ESEEM spectra that arise by modulation of an ^{14}N backbone amide group that is hydrogen bonded to a sulfur atom of Fe−S clusters (*33*−*35*).

DISCUSSION

Assignments of ^{14}N ESEEM. Because the FeMo-cofactor provides the site of N_2 reduction, its structure, electronic properties, and organization within the MoFe protein are of major importance. In the present work, we continue the efforts to identify the source of ^{14}N modulation of FeMo-cofactor by placing substitutions within its first shell of polypeptide interactions. To observe ^{14}N ESEEM from hyperfine-coupled ^{14}N to an electron-spin center, the ^{14}N nucleus should have electron-spin density on the nucleus, i.e, isotropic hyperfine coupling (*32*), as a result of some type of bonding interaction. This isotropic coupling combined with a small dipolar-interaction between the nuclear spin and the electron spin, and also the ^{14}N nuclear quadrupole coupling gives rise to the modulation. The MoFe protein X-ray structure reveals six candidates in the first shell that could either provide a hydrogen bond to a bridging sulfur atom within the FeMo-cofactor or be covalently bonded to the FeMo-cofactor and, thus, could give rise to the observed N1 and N2 ESEEM signatures described here. These are the side chains of α-442-histidine, α-96-arginine, α-195-histidine and α-359-arginine, plus the peptide NH groups of α-356-glycine and α-357-glycine (Figure 1, panels b and c) (*1, 9, 11*). In previous work, we found that substitution of the α-195-histidine residue by asparagine eliminates the major ^{14}N interaction with the $S = {}^3/_2$ spin system of FeMo-cofactor, denoted here N1, and results in an altered MoFe protein that can neither bind nor reduce the physiological substrate, N_2 (*15*). In contrast, substitution of the same residue by glutamine results in an altered MoFe protein that retains the wild-type N1 ESEEM signature. Furthermore, this α-195^{Gln} MoFe protein is able to bind N_2 but does not support appreciable N_2 reduction (*16, 17*). On the basis of these results, we concluded that the α-195-histidine residue does not directly contribute to the ESEEM signature (*15*). Rather, substitutions placed at the α-195 position appear to elicit small perturbations in FeMo-cofactor's polypeptide environment such that the NH−S bonding between FeMo-cofactor and its first shell of hydrogen-bonding interactions are affected. Thus, the major questions that emerged from previous work are concerned with the identification of the residue(s) directly responsible for ^{14}N modulation of FeMo-cofactor's spin $^3/_2$ system and whether such modulation is mechanistically significant.

We report here that substitution of the α-96-arginine residue by either glutamine or lysine results in an altered MoFe protein that retains the unperturbed wild-type N1 ESEEM pattern (Table 1). Considering the high sensitivity

Table 2: ^{14}N Hyperfine and Nuclear Quadrupole Coupling Tensors of Wild-Type, α-359^{Lys}, and α-381^{Leu} MoFe Proteins

MoFe protein (ESEEM pattern)	hyperfine coupling[a]		nuclear quadrupole coupling[a]		
	tensor (MHz)[b]	orientation (deg)	e^2qQ (MHz)	η	orientation (deg)[c]
wild-type (pattern N1)	0.98(3), 1.02(3), 1.14(9)	0, 0[d]	2.17(13)	0.59(7)	0, 0, 0
α-359^{Lys} (pattern N2$_a$)	0.4(1), 0.5(3), 0.4(3)	[e]	3.5(1)	0.35(5)	0, 60, 20
α-381^{Leu} (pattern N2$_b$)	0.4(1), 0.6(3), 0.4(3)	[e]	3.4(1)	0.40(5)	0, 60, 20

[a] The values in parentheses are the uncertainty limit in the last digits. [b] The tensor values are the intrinsic hyperfine coupling values (A_{int}) in the real spin, $S = 3/2$, representation (see Experimental Procedures). [c] Euler angles (α, β, γ) with respect to the **g**-tensor frame. The limit of uncertainty is ±10°. [d] Euler angles (ϕ, θ) with respect to the **g**-tensor frame. The limit of uncertainty is ±10°. Because the hyperfine tensor is mostly axial, Euler angles are defined by two rotations. [e] Because the anisotropic portion of the hyperfine tensor is small, **g** and the hyperfine tensors are set to be coaxial.

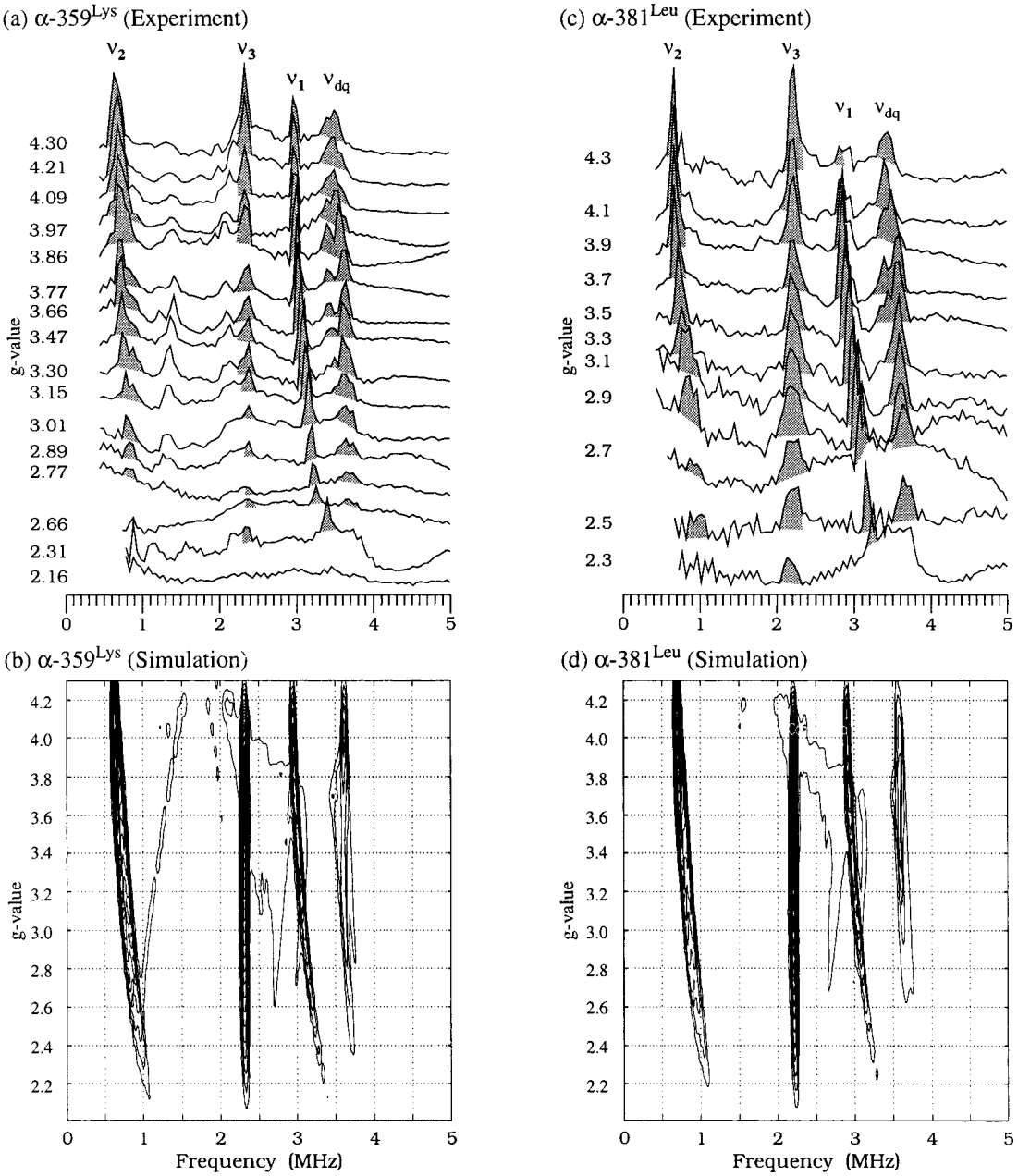

FIGURE 4: Field-dependent three-pulse ESEEM FT spectra obtained across the EPR spectra of the (a) α-359^{Lys} and (c) α-381^{Leu} MoFe proteins and (b, d) corresponding simulations. Experimental conditions: microwave frequency, (a) 9.640 and (b) 9.611 GHz; $\tau = 124-152$ ns. Simulation parameters are in Table 2 with $\tau = 150$ ns and a Gaussian line width of 0.05 MHz.

of ^{14}N ESEEM to the nuclear quadrupole coupling parameters, it is not possible that three electronically different nitrogens (guanidium in arginine, amine in lysine, and amide in glutamine) can elicit the same ^{14}N modulation. The α-96-arginine residue is, therefore, ruled out as the N1 modulation source.

Of the remaining candidates, two are the backbone amide nitrogens from α-356-glycine and α-357-glycine. Elimina-

tion of the N1 ESEEM spectrum in the α-359^{Lys} MoFe protein—and in certain other altered MoFe proteins (Table 1)—revealed the presence of a second, weak source of ^{14}N modulation (N2 ESEEM, Figures 2 and 4). The nuclear quadrupole coupling parameters originating from N2 are very different from those of N1 (Table 2). They are similar to those previously shown to arise by modulation of an ^{14}N backbone amide group that is hydrogen bonded to a sulfur atom of Fe−S clusters (*33*−*35*). We, therefore, propose that either or both of the amide nitrogens of α-356-glycine and α-357-glycine residues are the source of N2 modulation.

On the basis of these considerations, only α-359-arginine and α-442-histidine remain as candidates for the N1 modulation. We do not favor the latter because if α-442-histidine were the source of the N1 modulation, one would have to assume that all of the α-195^{Asn}, α-359^{Lys}, α-381^{Leu}, and α-381^{Ile} substitutions leave the $S = {}^3/_2$ EPR signal of the MoFe protein essentially unchanged, yet in effect cause the loss of α-442-histidine as a Mo ligand as evidenced by the loss of the N1 modulation. This assumption is not credible given our observation that replacement of the α-442-histidine by either asparagine or cysteine yields altered MoFe proteins that exhibit no $S = {}^3/_2$ EPR signal (Table 1). In addition, the absence of modulation for α-442-histidine is consistent with our suggestion that Mo is in the diamagnetic Mo(IV) oxidation state (*36*, *37*). Thus, by elimination, we propose the side chain of the α-359-arginine residue as the source of N1 modulation. This proposal is supported by the observation that substitution of α-359-arginine by lysine eliminated the deep N1 ESEEM pattern exhibited by the wild-type MoFe protein. If this assignment is correct, this report is the first observation of ESEEM from, and the first determination of the nuclear quadrupole coupling parameters for the terminal amine nitrogen of arginine.

Structural Implications. The FeMo-cofactor is covalently attached to the α-subunit of the MoFe protein only by coordination of α-275-cysteine and α-442-histidine to the apical metal ions, Fe and Mo, respectively (Figure 1c). Its spatial orientation may be controlled by any or all of five possible hydrogen-bond donors. These are the side chains of α-96-arginine and α-195-histidine, the amide NH groups of α-356-glycine and α-357-glycine, all of which putatively interact with the triangle of sulfides (S5, S2B, and S3A) comprising the central waist of the cluster, and the side chain of α-359-arginine, which putatively interacts with a sulfide (S4B) coordinated to Mo. In addition, the space between the three sulfides in the central waist region of the FeMo-cofactor is packed with the side chains of the above residues and with those of α-381-phenylalanine and α-70-valine (Figure 1b) (*1*, *9*, *11*). This information, together with the knowledge that the N1 and N2 ESEEM spectra arise through hydrogen bonds between the FeMo-cofactor and α-359-arginine (responsible for the N1 modulation) and between the FeMo-cofactor and α-356-glycine/α-357-glycine (responsible for the N2 modulation), respectively, allows several structural implications to be drawn.

First, substitution of α-359-arginine by lysine eliminates the N1 ESEEM originating from this residue without a new signal appearing from a hydrogen bond between and the lysine to the FeMo-cofactor (Table 1). However, substitution by glutamine apparently prevents FeMo-cofactor incorporation, which indicates that a positively charged residue at the α-359 position is necessary for FeMo-cofactor insertion. Second, the previous ESEEM measurements on MoFe proteins substituted at the α-195 position showed that, when α-195-histidine is replaced with asparagine, the FeMo-cofactor apparently reorients within the polypeptide matrix (*15*). We now interpret this reorientation as causing a perturbation of the hydrogen bond between α-359-arginine and sulfide S4B that results in the loss of the α-359-arginine modulation (N1) but does not affect the weak N2 modulation contributed by the amide NH groups of α-356-glycine/α-357-glycine. This sensitivity to changes at the α-195 residue supports the suggestion that α-195-histidine hydrogen bonds to the cluster, even though it gives no detectable ^{14}N modulation. Third, when α-96-arginine is substituted by either glutamine or lysine, the wild-type N1 ESEEM remains (Table 1). In the crystal structure of the *A. vinelandii* MoFe protein, the distance from the terminal amine nitrogen of α-96-arginine to sulfide S5 is the shortest (3.03 Å) among the five possible hydrogen bonds to the cluster. Nonetheless, any perturbation caused by substitution at the α-96-arginine residue is not sufficient to alter the N1 interaction arising from α-359-arginine.

In addition to substituting residues that are candidates to provide NH−S hydrogen bonds to the FeMo-cofactor, we also substituted the α-381-phenylalanine residue by leucine and isoleucine. These experiments were performed to determine if it is possible to indirectly alter the NH−S bonding pattern to the FeMo-cofactor by modifying a nonpolar R-group that appears to have a role in positioning FeMo-cofactor within its polypeptide pocket. We found that substitutions at the α-381 position eliminate the N1 interaction with FeMo-cofactor, indicating that such substitutions indirectly disrupt the hydrogen-bonding interaction between FeMo-cofactor and α-359-arginine (Table 1). The observation of the second kind of N2 ESEEM pattern, which results from substitution of α-381-phenylalanine by leucine and isoleucine (pattern $N2_b$, Table 2), also indicates a change in the proposed hydrogen bonding to FeMo-cofactor contributed by the backbone amides of α-356-glycine/α-357-glycine. Thus, it appears that steric influences from the substitution of the α-381-phenylalanine residue alter the nearby hydrogen bonds of α-195-histidine and/or α-356-glycine/α-357-glycine to permit the repositioning of FeMo-cofactor within its polypeptide pocket, such that significant hydrogen bonding within the first shell of FeMo-cofactor interactions is either altered or eliminated. This result is not surprising considering that α-381-phenylalanine closely approaches one face of FeMo-cofactor and, therefore, could constrain potential movement of the FeMo-cofactor within the polypeptide pocket (Figure 1).

In summary, ESEEM measurements on altered MoFe proteins suggest the following: (i) the side chain of the α-359-arginine is the source of the deep ESEEM N1 modulation; (ii) one or both of the amide nitrogens of α-356-glycine/α-357-glycine are responsible for the weak N2 modulation that is revealed when the N1 modulation is eliminated; (iii) the N1 modulation can be eliminated not only by substitution of the α-359-arginine residue, the proposed N1 source, but also by mutation of either the hydrogen-bonded α-195-histidine or the nonpolar α-381-phenylanine residue; these results indicate that the portions of residues α-195, α-359, and α-381 significantly influence

the positioning of the cofactor; (iv) although substitution at the α-195, α-359, or α-381 residues eliminates the N1 ESEEM signature, this loss is not correlated with the ability of the resulting MoFe protein to bind and reduce substrates. Thus, ESEEM can be used to detect slight reorientations of the FeMo-cofactor within its polypeptide pocket, but the loss (or perturbation) of the first shell of hydrogen-bonding interactions between the FeMo-cofactor and its polypeptide environment, as detected by ESEEM, has yet to be proved mechanistically relevant.

REFERENCES

1. Chan, M. K., Kim, J., and Rees, D. C. (1993) *Science 260*, 792−794.
2. Peters, J. W., Stowell, M. H. B., Soltis, S. M., Finnegan, M. G., Johnson, M. K., and Rees, D. C. (1997) *Biochemistry 36*, 1181−1187.
3. Peters, J. W., Fisher, K., Newton, W., and Dean, D. R. (1995) *J. Biol. Chem. 270*, 27007−27013.
4. Lanzilotta, W. N., and Seefeldt, L. C. (1996) *Biochemistry 35*, 16770−16776.
5. Schindelin, H., Kisker, C., Schlessman, J. L., Howard, J. B., and Rees, D. C. (1997) *Nature 387*, 370−376.
6. Shah, V. K., and Brill, W. J. (1977) *Proc. Natl. Acad. Sci. U.S.A. 74*, 3249−3253.
7. Scott, D. J., May, H. D., Newton, W. E., Brigle, K. E., and Dean, D. R. (1990) *Nature 343*, 188−190.
8. Burgess, B. K., and Lowe, D. L. (1996) *Chem. Rev. 96*, 2983−3011.
9. Howard, J. B., and Rees, D. C. (1996) *Chem. Rev. 96*, 2965−2982.
10. Seefeldt, L. C., and Dean, R. D. (1997) *Acc. Chem. Res. 30*, 260−266.
11. Kim, J., and Rees, D. C. (1992) *Nature 360*, 553−560.
12. Dikanov, S. A., and Tsvetkov, Y. D. (1992) *Electron Spin−Echo Envelope Modulation (ESEEM) Spectroscopy*, CRC Press, Boca Raton, FL.
13. Thomann, H., Morgan, T. V., Jin, H., Burgmayer, S. J. N., Bare, R. E., and Stiefel, E. I. (1987) *J. Am. Chem. Soc. 109*, 7913−7914.
14. Thomann, H., Bernardo, M., Newton, W. E., and Dean, D. R. (1991) *Proc. Natl. Acad. Sci. U.S.A. 88*, 6620−6623.
15. DeRose, V. J., Kim, C.-H., Newton, W. E., Dean, D. R., and Hoffman, B. M. (1995) *Biochemistry 34*, 2809−2814.
16. Kim, C.-H., Newton, W. E., and Dean, D. R. (1995) *Biochemistry 35*, 2798−2808.
17. Dilworth, M. J., and Fisher, K. (1998) *Anal. Biochem. 256*, 242−244.
18. Brigle, K. E., Weiss, M. C., Newton, W. E., and Dean, D. R. (1987) *J. Bacteriol. 169*, 1547−1553.
19. Brigle, K. E., Setterquist, R. A., Dean, D. R., Cantwell, J. S., Weiss, M. C., and Newton, W. E. (1987) *Proc. Natl. Acad. Sci. U.S.A. 84*, 7066−7069.
20. Shen, J., Dean, D. R., and Newton, W. E. (1997) *Biochemistry 36*, 4884−4894.
21. Feher, G. (1959) *Phys. Rev. 114*, 1219−1244.
22. Mailer, C., and Taylor, C. P. S. (1973) *Biochim. Biophys. Acta 322*, 195−203.
23. Werst, M. M., Davoust, C. E., and Hoffman, B. M. (1991) *J. Am. Chem. Soc. 113*, 1533−1538.
24. Fan, C., Doan, P. E., Davoust, C. E., and Hoffman, B. M. (1992) *J. Magn. Res. 98*, 62−72.
25. Mims, W. B. (1984) *J. Magn. Res. 59*, 291−306.
26. Hoffman, B. M., Gurbiel, R. J., Werst, M. M., and Sivaraja, M. (1989) in *Advanced EPR. Applications in Biochemistry* (Hoff, A. J., Ed.), pp 541−591, Elsevier, Amsterdam.
27. True, A. E., Nelson, M. J., Venters, R. A., Orme-Johnson, W. H., and Hoffman, B. M. (1988) *J. Am. Chem. Soc. 110*, 1935−1943.
28. True, A. E., McLean, P., Nelson, M. J., Orme-Johnson, W. H., and Hoffman, B. M. (1990) *J. Am. Chem. Soc. 112*, 651−657.
29. Astashkin, A. V., Dikanov, S. A., and Tsvetkov, Y. D. (1984) *Zh. Strukt. Khim. 25*, 53−64.
30. Hoffman, B. M., DeRose, V. J., Doan, P. E., Gurbiel, R. J., Houseman, A. L. P., and Telser, J. (1993) in *Biological Magnetic Resonance* (Berliner, L. J., and Reuben, J., Eds.) Vol. 13, Plenum Press, New York.
31. Muha, G. M. (1982) *J. Magn. Res. 49*, 431−443.
32. Lee, H.-I., Doan, P. E., and Hoffman, B. M. (1998) (Manuscript in preparation).
33. Dikanov, S. A., Tyryshkin, A. M., Felli, I., Reijerse, E. J., and Hüttermann, J. (1995) *J. Magn. Res. 108*, 99−102.
34. Shergill, J. K., and Cammack, R. (1994) *Biochem. Biophys. Acta 1185*, 43−49.
35. Cammack, R., Chapman, A., McCracken, J., and Peisach, J. (1991) *J. Chem. Soc., Faraday Trans. 87*, 3203−3206.
36. Venters, R. A., Nelson, M. J., McLean, P. A., True, A. E., Levy, M. A., Hoffman, B. M., and Orme-Johnson, W. H. (1986) *J. Am. Chem. Soc. 108*, 3487−3498.
37. Lee, H.-I., Hales, B. J., and Hoffman, B. M. (1997) *J. Am. Chem. Soc. 119*, 11395−11400.
38. Kim, J., and Rees, D. C. (1992) *Science 257*, 1677−1682.
39. Kim, J., Woo., D., and Rees, D. C. (1993) *Biochemistry 32*, 7104−7115.

BI980956A